Available online at www.sciencedirect.com

SCIENCE DIRECT®

European Journal of Mechanics A/Solids 24 (2005) 253–262

EUROPEAN JOURNAL OF MECHANICS A/SOLIDS

The dynamic behavior of two collinear interface cracks in magneto-electro-elastic materials

Zhen-Gong Zhou, Lin-Zhi Wu, Biao Wang

P.O. Box 1247, Center for Composite Materials, Harbin Institute of Technology, Harbin, 150001, PR China

Received 12 July 2004; accepted 7 October 2004

Available online 28 December 2004

Abstract

In this paper, the dynamic behavior of two collinear symmetric interface cracks between two dissimilar magneto-electro-elastic material half planes under the harmonic anti-plane shear waves loading is investigated by Schmidt method. By using the Fourier transform, the problem can be solved with a set of triple integral equations in which the unknown variable is the jump of the displacements across the crack surfaces. To solve the triple integral equations, the jump of the displacements across the crack surface is expanded in a series of Jacobi polynomials. Numerical solutions of the stress intensity factor, the electric displacement intensity factor and the magnetic flux intensity factor are given. The relations among the electric filed, the magnetic flux field and the stress field are obtained.

Keywords: Magneto-electro-elastic materials; Interface crack; Triple integral equations

1. Introduction

Composite material consisting of a piezoelectric phase and a piezomagnetic phase has drawn significant interest in recent years, due to the rapid development in adaptive material systems. In some cases, the coupling effect of piezoelectric/piezomagnetic composites can be even obtained a hundred times larger than that in a single-phase magnetoelectric material. Consequently, they are extensively used as electric packaging, sensors and actuators, e.g., magnetic field probes, acoustic/ultrasonic devices, hydrophones, and transducers with the responsibility of electro-magneto-mechanical energy conversion (Wu and Huang, 2000). With increasingly wide application of piezoelectric and piezomagnetic composites in smart systems, cavity or crack problems in magnetoelectroelastic media have received considerable interest. When subjected to mechanical, magnetic and electrical loads in service, these magneto-electro-elastic materials can fail prematurely due to some defects, e.g. cracks, holes, etc. arising during their manufacturing process. Therefore, it is of great importance to study the magneto-electro-elastic interaction and dynamic fracture behavior of magneto-electro-elastic materials (Sih and Song, 2003; Song and Sih, 2003; Wang and Mai, 2003; Gao et al., 2003d, 2003a; Spyropoulos et al., 2003). Liu et al. (2001) studied the generalized 2D problem of an infinite magnetoelectroelastic plane with an elliptical hole. Gao et al. (2003b; 2003c), Wang and Mai (2004) also studied the fracture problem of the piezoelectric/piezomagnetic materials. The static fracture behavior of two collinear cracks in the piezoelectric material has been investigated by Zhou et al. (2001). More recently, Zhou et al. (2004) considered the static fracture problem of the piezoelectric/piezomagnetic materials for the collinear symmetric interface cracks.

E-mail address: zhouzhg@hit.edu.cn (Z.-G. Zhou).

0997-7538/$ – see front matter
doi:10.1016/j.euromechsol.2004.10.006

The development of piezoelectric-piezomagnetic materials has its roots in the early work of Van Suchtelen (1972) who proposed that the combination of piezoelectric-piezomagnetic phases may exhibit a new material property—the magnetoelectric coupling effect. Since then, there have not been many researchers studying magnetoelectric coupling effect in $BaTiO_3$–$CoFe_2O_4$ composites, and most research results published were obtained in recent years (Wu and Huang, 2000; Sih and Song, 2003; Song and Sih, 2003; Wang and Mai, 2003; Gao et al., 2003d, 2003a; Spyropoulos et al., 2003; Liu et al., 2001; Gao et al., 2003b, 2003c; Wang and Mai, 2003; Harshe et al., 1993; Avellaneda and Harshe, 1994; Nan, 1994; Benveniste, 1995; Huang and Kuo, 1997; Li, 2000; Zhou et al., 2004). However, relatively few works have been made for the dynamic fracture analysis in the magneto-electro-elastic materials due to the mathematical complexities. To our knowledge, the magneto-electro-elastic dynamic behavior of magneto-electro-elastic materials with two collinear symmetric interface cracks subjected to the harmonic anti-plane shear waves has not been studied.

In this paper, the dynamic behavior of two collinear interface cracks between two dissimilar magneto-electro-elastic material half planes subjected to the harmonic anti-plane shear waves is investigated by use of an appropriate method, namely the Schmidt method (Morse and Feshbach, 1958; Yan, 1967). The static solution in the reference (Zhou et al., 2004) is a limiting procedure from the dynamic solution in the present paper. The Fourier transform is applied and a mixed boundary value problem is reduced to a triple integral equations. To solve the triple integral equations, the jump of the displacements across the crack surfaces is expanded in a series of Jacobi polynomials. This process is quite different from those adopted in the references (Sih and Song, 2003; Song and Sih, 2003; Wang and Mai, 2003; Gao et al., 2003d, 2003a; Spyropoulos et al., 2003; Liu et al., 2001; Gao et al., 2003b, 2003c; Wang and Mai, 2003) as mentioned above. Numerical solutions are obtained for the stress, the electric displacement and the magnetic flux intensity factors.

2. Formulation of the problem

It is assumed that there are two collinear interface cracks of length $1-b$ between two dissimilar magneto-electro-elastic material half planes as shown in Fig. 1. $2b$ is the distance between two cracks (the solution of two collinear interface cracks of length $a-b$ in the magneto-electro-elastic materials can easily be obtained by a simple change in the numerical values of the present paper for crack length $1-b/a$, $a>b>0$). In this paper, the harmonic elastic anti-plane shear stress wave is vertically incident. Let ω be the circular frequency of the incident wave. $-\tau_0$ is a magnitude of the incident wave. In what follows, the time dependence of all field quantities assumed to be of the form $e^{-i\omega t}$ will be suppressed but understood. The piezoelectric/piezomagnetic boundary-value problem for anti-plane shear is considerably simplified if we consider only the out-of-plane displacement, the in-plane electric and the in-plane magnetic fields. As discussed in Soh's (Soh et al., 2000) works, since no opening displacement exists for the present anti-plane problem, the crack surfaces can be assumed to be in perfect contact. Accordingly, the electric and magnetic potential, the normal electric displacement and the normal magnetic flux are assumed to be continuous across the crack surfaces. So the boundary conditions of the present problem are (In this paper, we just consider the perturbation fields.):

$$\begin{cases} \tau_{yz}^{(1)}(x,0^+)=\tau_{yz}^{(2)}(x,0^-)=-\tau_0, & b\leqslant|x|\leqslant 1, \\ w^{(1)}(x,0^+)=w^{(2)}(x,0^-), & |x|<b,\ |x|>1, \end{cases} \tag{1}$$

$$\phi^{(1)}(x,0^+)=\phi^{(2)}(x,0^-), \quad D_y^{(1)}(x,0^+)=D_y^{(2)}(x,0^-), \quad |x|\leqslant\infty, \tag{2}$$

$$\psi^{(1)}(x,0^+)=\psi^{(2)}(x,0^-), \quad B_y^{(1)}(x,0^+)=B_y^{(2)}(x,0^-), \quad |x|\leqslant\infty, \tag{3}$$

$$w^{(1)}(x,y)=w^{(2)}(x,y)=0 \quad \text{for } (x^2+y^2)^{1/2}\to\infty, \tag{4}$$

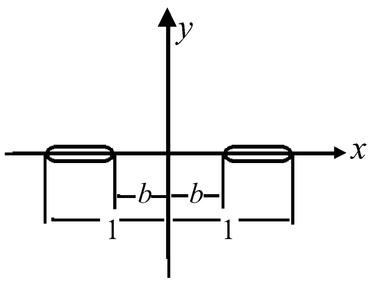

Fig. 1. Two interface cracks between two dissimilar magneto-electro-elastic materials half planes.

where $\tau_{zk}^{(i)}$, $D_k^{(i)}$ and $B_k^{(i)}$ ($k = x, y$, $i = 1, 2$) are the anti-plane shear stress, in-plane electric displacement and in-plane magnetic flux, respectively. $w^{(i)}$, $\phi^{(i)}$ and $\psi^{(i)}$ are the mechanical displacement, the electric potential and the magnetic potential, respectively. Note that all quantities with superscript i ($i = 1, 2$) refer to the upper half plane and the lower half plane as in Fig. 1, respectively. In this paper, we only consider that τ_0 is positive.

It is assumed that the magneto-electro-elastic material is transversely isotropic. So the constitutive equations for the mode III crack in the magneto-electro-elastic material can be expressed as

$$\tau_{zk}^{(i)} = c_{44}^{(i)} w^{(i)}{}_{,k} + e_{15}^{(i)} \phi^{(i)}{}_{,k} + q_{15}^{(i)} \psi^{(i)}{}_{,k} \quad (k = x, y,\ i = 1, 2), \tag{5}$$

$$D_k^{(i)} = e_{15}^{(i)} w^{(i)}{}_{,k} - \varepsilon_{11}^{(i)} \phi^{(i)}{}_{,k} - d_{11}^{(i)} \psi^{(i)}{}_{,k} \quad (k = x, y,\ i = 1, 2), \tag{6}$$

$$B_k^{(i)} = q_{15}^{(i)} w^{(i)}{}_{,k} - d_{11}^{(i)} \phi^{(i)}{}_{,k} - \mu_{11}^{(i)} \psi^{(i)}{}_{,k} \quad (k = x, y,\ i = 1, 2), \tag{7}$$

where $c_{44}^{(i)}$ is shear modulus, $e_{15}^{(i)}$ is piezoelectric coefficient, $\varepsilon_{11}^{(i)}$ is dielectric parameter, $q_{15}^{(i)}$ is piezomagnetic coefficient, $d_{15}^{(i)}$ is electromagnetic coefficient, $\mu_{11}^{(i)}$ is magnetic permeability.

The anti-plane governing equations are

$$c_{44}^{(i)} \nabla^2 w^{(i)} + e_{15}^{(i)} \nabla^2 \phi^{(i)} + q_{15}^{(i)} \nabla^2 \psi^{(i)} = \rho^{(i)} \frac{\partial^2 w^{(i)}}{\partial t^2} \quad (i = 1, 2), \tag{8}$$

$$e_{15}^{(i)} \nabla^2 w^{(i)} - \varepsilon_{11}^{(i)} \nabla^2 \phi^{(i)} - d_{11}^{(i)} \nabla^2 \psi^{(i)} = 0 \quad (i = 1, 2), \tag{9}$$

$$q_{15}^{(i)} \nabla^2 w^{(i)} - d_{11}^{(i)} \nabla^2 \phi^{(i)} - \mu_{11}^{(i)} \nabla^2 \psi^{(i)} = 0 \quad (i = 1, 2), \tag{10}$$

where $\nabla^2 = \partial^2/\partial x^2 + \partial^2/\partial y^2$ is the two-dimensional Laplace operator. $\rho^{(i)}$ is the density of the piezoelectric/piezomagnetic materials. Because of the assumed symmetry in geometry and loading, it is sufficient to consider the problem for $0 \leqslant x < \infty$, $-\infty \leqslant y < \infty$ only. A Fourier transform is applied to Eqs. (8)–(10). It is assumed that the solutions are

$$\begin{cases} w^{(1)}(x, y) = \dfrac{2}{\pi} \displaystyle\int_0^\infty A_1(s)\, \mathrm{e}^{-\gamma_1 y} \cos(sx)\, \mathrm{d}s, \\ \phi^{(1)}(x, y) = \dfrac{a_1}{a_0} w^{(1)}(x, y) + \dfrac{2}{\pi} \displaystyle\int_0^\infty B_1(s)\, \mathrm{e}^{-sy} \cos(sx)\, \mathrm{d}s \quad (y \geqslant 0), \\ \psi^{(1)}(x, y) = \dfrac{a_2}{a_0} w^{(1)}(x, y) + \dfrac{2}{\pi} \displaystyle\int_0^\infty C_1(s)\, \mathrm{e}^{-sy} \cos(sx)\, \mathrm{d}s, \end{cases} \tag{11}$$

$$\begin{cases} w^{(2)}(x, y) = \dfrac{2}{\pi} \displaystyle\int_0^\infty A_2(s)\, \mathrm{e}^{\gamma_2 y} \cos(sx)\, \mathrm{d}s, \\ \phi^{(2)}(x, y) = \dfrac{a_4}{a_3} w^{(2)}(x, y) + \dfrac{2}{\pi} \displaystyle\int_0^\infty B_2(s)\, \mathrm{e}^{sy} \cos(sx)\, \mathrm{d}s \quad (y \leqslant 0), \\ \psi^{(2)}(x, y) = \dfrac{a_5}{a_3} w^{(2)}(x, y) + \dfrac{2}{\pi} \displaystyle\int_0^\infty C_2(s)\, \mathrm{e}^{sy} \cos(sx)\, \mathrm{d}s, \end{cases} \tag{12}$$

where $A_1(s)$, $B_1(s)$, $C_1(s)$, $A_2(s)$, $B_2(s)$ and $C_2(s)$ are unknown functions.

$$\gamma_1^2 = s^2 - \omega^2/c_1^2, \quad c_1^2 = \mu^{(1)}/\rho^{(1)}, \quad \mu^{(1)} = c_{44}^{(1)} + \frac{a_1 e_{15}^{(1)}}{a_0} + \frac{a_2 q_{15}^{(1)}}{a_0}, \quad a_0 = \varepsilon_{11}^{(1)} \mu_{11}^{(1)} - d_{11}^{(1)2},$$
$$a_1 = \mu_{11}^{(1)} e_{15}^{(1)} - d_{11}^{(1)} q_{15}^{(1)}, \quad a_2 = q_{15}^{(1)} \varepsilon_{11}^{(1)} - d_{11}^{(1)} e_{15}^{(1)}, \quad \gamma_2^2 = s^2 - \omega^2/c_2^2, \quad c_2^2 = \mu^{(2)}/\rho^{(2)},$$
$$\mu^{(2)} = c_{44}^{(2)} + \frac{a_4 e_{15}^{(2)}}{a_3} + \frac{a_5 q_{15}^{(2)}}{a_3}, \quad a_3 = \varepsilon_{11}^{(2)} \mu_{11}^{(2)} - d_{11}^{(2)2}, \quad a_4 = \mu_{11}^{(2)} e_{15}^{(2)} - d_{11}^{(2)} q_{15}^{(2)}, \quad a_5 = q_{15}^{(2)} \varepsilon_{11}^{(2)} - d_{11}^{(2)} e_{15}^{(2)}.$$

It can be obtained $\gamma_1 = \gamma_2 = s$ for $\omega = 0$. Hence, the solutions of $w^{(i)}(x, y)$, $\phi^{(i)}(x, y)$ and $\psi^{(i)}(x, y)$ in Eqs. (11), (12) will be the same as the static solutions in the reference (Zhou et al., 2004) for $\omega = 0$.

So from Eqs. (5)–(7), we have

$$\tau_{yz}^{(1)}(x,y) = -\frac{2}{\pi}\int_0^\infty \left\{\gamma_1\mu^{(1)}A_1(s)\,\mathrm{e}^{-\gamma_1 y} + s\left[e_{15}^{(1)}B_1(s) + q_{15}^{(1)}C_1(s)\right]\mathrm{e}^{-sy}\right\}\cos(sx)\,\mathrm{d}s, \tag{13}$$

$$D_y^{(1)}(x,y) = \frac{2}{\pi}\int_0^\infty s\left[\varepsilon_{11}^{(1)}B_1(s) + d_{11}^{(1)}C_1(s)\right]\mathrm{e}^{-sy}\cos(sx)\,\mathrm{d}s, \tag{14}$$

$$B_y^{(1)}(x,y) = \frac{2}{\pi}\int_0^\infty s\left[d_{11}^{(1)}B_1(s) + \mu_{11}^{(1)}C_1(s)\right]\mathrm{e}^{-sy}\cos(sx)\,\mathrm{d}s, \tag{15}$$

$$\tau_{yz}^{(2)}(x,y) = \frac{2}{\pi}\int_0^\infty \left\{\gamma_2\mu^{(2)}A_2(s)\,\mathrm{e}^{\gamma_2 y} + s\left[e_{15}^{(2)}B_2(s) + q_{15}^{(2)}C_2(s)\right]\mathrm{e}^{sy}\right\}\cos(sx)\,\mathrm{d}s, \tag{16}$$

$$D_y^{(2)}(x,y) = -\frac{2}{\pi}\int_0^\infty s\left[\varepsilon_{11}^{(2)}B_2(s) + d_{11}^{(2)}C_2(s)\right]\mathrm{e}^{sy}\cos(sx)\,\mathrm{d}s, \tag{17}$$

$$B_y^{(2)}(x,y) = -\frac{2}{\pi}\int_0^\infty s\left[d_{11}^{(2)}B_2(s) + \mu_{11}^{(2)}C_2(s)\right]\mathrm{e}^{sy}\cos(sx)\,\mathrm{d}s. \tag{18}$$

To solve the problem, the jump of the displacements across the crack surfaces is defined as follows:

$$f(x) = w^{(1)}(x,0^+) - w^{(2)}(x,0^-). \tag{19}$$

Substituting Eqs. (11), (12) into Eq. (19), and applying the Fourier transform and the boundary conditions, it can be obtained

$$\bar{f}(s) = A_1(s) - A_2(s), \tag{20}$$

$$\frac{a_1}{a_0}A_1(s) - \frac{a_4}{a_3}A_2(s) + B_1(s) - B_2(s) = 0, \tag{21}$$

$$\frac{a_2}{a_0}A_1(s) - \frac{a_5}{a_3}A_2(s) + C_1(s) - C_2(s) = 0. \tag{22}$$

Substituting Eqs. (13)–(18) into Eqs. (1)–(3), it can be obtained

$$\mu^{(1)}\gamma_1 A_1(s) + se_{15}^{(1)}B_1(s) + sq_{15}^{(1)}C_1(s) + \mu^{(2)}\gamma_2 A_2(s) + se_{15}^{(2)}B_2(s) + sq_{15}^{(2)}C_2(s) = 0, \tag{23}$$

$$\varepsilon_{11}^{(1)}B_1(s) + d_{11}^{(1)}C_1(s) + \varepsilon_{11}^{(2)}B_2(s) + d_{11}^{(2)}C_2(s) = 0, \tag{24}$$

$$d_{11}^{(1)}B_1(s) + \mu_{11}^{(1)}C_1(s) + d_{11}^{(2)}B_2(s) + \mu_{11}^{(2)}C_2(s) = 0. \tag{25}$$

By solving six Eqs. (20)–(25) with six unknown functions $A_1(s)$, $B_1(s)$, $C_1(s)$, $A_2(s)$, $B_2(s)$, $C_2(s)$ and applying the boundary condition (1) to the results, it can be obtained:

$$\frac{2}{\pi}\int_0^\infty g_1(s)\bar{f}(s)\cos(sx)\,\mathrm{d}s = -\tau_0, \quad b \leqslant x \leqslant 1, \tag{26}$$

$$\int_0^\infty \bar{f}(s)\cos(sx)\,\mathrm{d}s = 0, \quad 0 < x < b,\ x > 1, \tag{27}$$

where $g_1(s)$ is a known function (see Appendix). $\lim_{s\to\infty} g_1(s)/s = \beta_1$. Where β_1 is a constant which depends on the properties of the materials (see Appendix). When the properties of the upper and the lower half planes is the same, $\beta_1 = -c_{44}^{(1)}/2$. To determine the unknown functions $\bar{f}(s)$, the triple integral equations (26), (27) must be solved.

3. Solution of the triple integral equations

From the natural property of the displacement along the crack line, it can be obtained that the jump of the displacements across the crack surface is a finite, continuous and differentiable function. Hence, the jump of the displacements across the crack surfaces can be represented by the following series:

$$f(x)=\sum_{n=0}^{\infty} b_n P_n^{(1/2,1/2)}\left(\frac{x-(1+b)/2}{(1-b)/2}\right)\left(1-\frac{(x-(1+b)/2)^2}{((1-b)/2)^2}\right)^{1/2}, \quad \text{for } b \leqslant x \leqslant 1, \tag{28}$$

where b_n is unknown coefficients to be determined and $P_n^{(1/2,1/2)}(x)$ is a Jacobi polynomial (Gradshteyn and Ryzhik, 1980). The Fourier transform of Eq. (28) are (Erdelyi, 1954)

$$\bar{f}(s)=\sum_{n=0}^{\infty} b_n F_n G_n(s)\frac{1}{s}J_{n+1}\left(s\frac{1-b}{2}\right), \tag{29}$$

$$F_n=2\sqrt{\pi}\frac{\Gamma(n+1+1/2)}{n!}, \qquad G_n(s)=\begin{cases}(-1)^{n/2}\cos\left(s\dfrac{1+b}{2}\right), & n=0,2,4,6,\ldots,\\ (-1)^{(n+1)/2}\sin\left(s\dfrac{1+b}{2}\right), & n=1,3,5,7,\ldots,\end{cases} \tag{30}$$

where $\Gamma(x)$ and $J_n(x)$ are the Gamma and Bessel functions, respectively.

Substituting Eq. (29) into Eqs. (26), (27), Eq. (27) has been automatically satisfied. After integration with respect to x in $[b,x]$, Eq. (26) reduces to

$$\sum_{n=0}^{\infty} b_n F_n \int_0^{\infty} \frac{g_1(s)}{s^2} G_n(s) J_{n+1}\left(s\frac{1-b}{2}\right)\left[\sin(sx)-\sin(sb)\right] \mathrm{d}s=-\frac{\pi\tau_0}{2}(x-b). \tag{31}$$

From the relationship (Gradshteyn and Ryzhik, 1980),

$$\int_0^{\infty}\frac{1}{s}J_n(sa)\sin(bs)\,\mathrm{d}s=\begin{cases}\dfrac{\sin[n\sin^{-1}(b/a)]}{n}, & a>b,\\ \dfrac{a^n\sin(n\pi/2)}{n[b+\sqrt{b^2-a^2}]^n}, & a<b,\end{cases} \tag{32}$$

$$\int_0^{\infty}\frac{1}{s}J_n(sa)\cos(bs)\,\mathrm{d}s=\begin{cases}\dfrac{\cos[n\sin^{-1}(b/a)]}{n}, & a>b,\\ \dfrac{a^n\cos(n\pi/2)}{n[b+\sqrt{b^2-a^2}]^n}, & a<b\end{cases} \tag{33}$$

the semi-infinite integral in Eq. (31) can be modified as

$$\begin{aligned}&\int_0^{\infty}\frac{1}{s}\left\{\beta_1+\left[\frac{g_1(s)}{s}-\beta_1\right]\right\}J_{n+1}\left(s\frac{1-b}{2}\right)\cos\left(s\frac{1+b}{2}\right)\sin(sx)\,\mathrm{d}s\\ &\quad=\frac{\beta_1}{2(n+1)}\left\{\frac{((1-b)/2)^{n+1}\sin((n+1)\pi/2)}{\{x+(1+b)/2+\sqrt{(x+(1+b)/2)^2-((1-b)/2)^2}\}^{n+1}}-\sin\left[(n+1)\sin^{-1}\left(\frac{1+b-2x}{1-b}\right)\right]\right\}\\ &\qquad+\int_0^{\infty}\frac{1}{s}\left[\frac{g_1(s)}{s}-\beta_1\right]J_{n+1}\left(s\frac{1-b}{2}\right)\cos\left(s\frac{1+b}{2}\right)\sin(sx)\,\mathrm{d}s,\end{aligned} \tag{34}$$

$$\begin{aligned}&\int_0^{\infty}\frac{1}{s}\left\{\beta_1+\left[\frac{g_1(s)}{s}-\beta_1\right]\right\}J_{n+1}\left(s\frac{1-b}{2}\right)\sin\left(s\frac{1+b}{2}\right)\sin(sx)\,\mathrm{d}s\\ &\quad=\frac{\beta_1}{2(n+1)}\left\{\cos\left[(n+1)\sin^{-1}\left(\frac{1+b-2x}{1-b}\right)\right]-\frac{((1-b)/2)^{n+1}\cos((n+1)\pi/2)}{\{x+(1+b)/2+\sqrt{(x+(1+b)/2)^2-((1-b)/2)^2}\}^{n+1}}\right\}\\ &\qquad+\int_0^{\infty}\frac{1}{s}\left[\frac{g_1(s)}{s}-\beta_1\right]J_{n+1}\left(s\frac{1-b}{2}\right)\sin\left(s\frac{1+b}{2}\right)\sin(sx)\,\mathrm{d}s.\end{aligned} \tag{35}$$

It can be seen that the integrands in the right end of Eqs. (34), (35) tend rapidly to zero. Thus the semi-infinite integrals in Eqs. (34), (35) can be numerical evaluated easily. Eq. (31) can now be solved for the coefficients b_n by the Schmidt method (Morse and Feshbach, 1958; Yan, 1967). The method is omitted in the present work. It can be seen in references (Zhou et al., 1999a, 1999b; 2001).

4. Intensity factors

The coefficients b_n are known, so that the entire perturbation stress field, the perturbation electric displacement and the magnetic flux can be obtained. However, in fracture mechanics, it is of importance to determine the perturbation stress $\tau_{yz}^{(1)}$, the perturbation electric displacement $D_y^{(1)}$ and the magnetic flux $B_y^{(1)}$ in the vicinity of the crack tips. In the case of the present study, $\tau_{yz}^{(1)}$, $D_y^{(1)}$ and $B_y^{(1)}$ along the crack line can be expressed respectively as

$$\tau_{yz}^{(1)}(x,0)=\frac{2}{\pi}\sum_{n=0}^{\infty}b_nF_n\int_0^{\infty}\frac{g_1(s)}{s}G_n(s)J_{n+1}\left(s\frac{1-b}{2}\right)\cos(xs)\,\mathrm{d}s, \tag{36}$$

$$D_y^{(1)}(x,0)=\frac{2}{\pi}\sum_{n=0}^{\infty}b_nF_n\int_0^{\infty}\frac{g_2(s)}{s}G_n(s)J_{n+1}\left(s\frac{1-b}{2}\right)\cos(xs)\,\mathrm{d}s, \tag{37}$$

$$B_y^{(1)}(x,0)=\frac{2}{\pi}\sum_{n=0}^{\infty}b_nF_n\int_0^{\infty}\frac{g_3(s)}{s}G_n(s)J_{n+1}\left(s\frac{1-b}{2}\right)\cos(xs)\,\mathrm{d}s, \tag{38}$$

where $g_2(s)$ and $g_3(s)$ are known functions (see Appendix). $\lim_{s\to\infty} g_2(s)/s=\beta_2$, $\lim_{s\to\infty} g_3(s)/s=\beta_3$. Where β_2 and β_3 are two constants which depend on the properties of the materials (see Appendix). When the properties of the upper and the lower half planes is the same, $\beta_2=-e_{15}^{(1)}/2$ and $\beta_3=-q_{15}^{(1)}/2$. As discussed in reference (Zhou et al., 2004), the singular parts of the stress field, the electric displacement and the magnetic flux can be expressed respectively as follows ($x>1$ or $x<b$):

$$\tau=\frac{\beta_1}{\pi}\sum_{n=0}^{\infty}b_nF_nH_n(b,x), \tag{39}$$

$$D=\frac{\beta_2}{\pi}\sum_{n=0}^{\infty}b_nF_nH_n(b,x), \tag{40}$$

$$B=\frac{\beta_3}{\pi}\sum_{n=0}^{\infty}b_nF_nH_n(b,x), \tag{41}$$

where

$$H_n(b,x)=\begin{cases}(-1)^{n+1}R(b,x,n), & 0<x<b,\\ -R(b,x,n), & x>1,\end{cases}$$

$$R(b,x,n)=\frac{2(1-b)^{n+1}}{\sqrt{|1+b-2x|^2-(1-b)^2}\left[|1+b-2x|+\sqrt{|1+b-2x|^2-(1-b)^2}\right]^{n+1}}.$$

At the left tip of the right crack, we obtain the stress intensity factor K_L as

$$K_\mathrm{L}=\lim_{x\to b^-}\sqrt{2(b-x)}\cdot\tau=-\frac{\beta_1}{\pi}\sqrt{\frac{2}{1-b}}\sum_{n=0}^{\infty}(-1)^nb_nF_n. \tag{42}$$

At the right tip of the right crack, we obtain the stress intensity factor K_R as

$$K_\mathrm{R}=\lim_{x\to 1^+}\sqrt{2(x-1)}\cdot\tau=-\frac{\beta_1}{\pi}\sqrt{\frac{2}{1-b}}\sum_{n=0}^{\infty}b_nF_n. \tag{43}$$

At the left tip of the right crack, we obtain the electric displacement intensity factor K_{L}^{D} as

$$K_{\mathrm{L}}^{D}=\lim_{x\to b^-}\sqrt{2(b-x)}\cdot D=-\frac{\beta_2}{\pi}\sqrt{\frac{2}{1-b}}\sum_{n=0}^{\infty}(-1)^n b_n F_n=\frac{\beta_2}{\beta_1}K_{\mathrm{L}}. \tag{44}$$

At the right tip of the right crack, we obtain the electric displacement intensity factor K_{R}^{D} as

$$K_{\mathrm{R}}^{D}=\lim_{x\to 1^+}\sqrt{2(x-1)}\cdot D=-\frac{\beta_2}{\pi}\sqrt{\frac{2}{1-b}}\sum_{n=0}^{\infty}b_n F_n=\frac{\beta_2}{\beta_1}K_{\mathrm{R}}. \tag{45}$$

At the left tip of the right crack, we obtain the magnetic flux intensity factor K_{L}^{B} as

$$K_{\mathrm{L}}^{B}=\lim_{x\to b^-}\sqrt{2(b-x)}\cdot B=-\frac{\beta_3}{\pi}\sqrt{\frac{2}{1-b}}\sum_{n=0}^{\infty}(-1)^n b_n F_n=\frac{\beta_3}{\beta_1}K_{\mathrm{L}}. \tag{46}$$

At the right tip of the right crack, we obtain the magnetic flux intensity factor K_{R}^{B} as

$$K_{\mathrm{R}}^{B}=\lim_{x\to 1^+}\sqrt{2(x-1)}\cdot D=-\frac{\beta_3}{\pi}\sqrt{\frac{2}{1-b}}\sum_{n=0}^{\infty}b_n F_n=\frac{\beta_3}{\beta_1}K_{\mathrm{R}}. \tag{47}$$

5. Conclusions

As discussed in the works (Zhou et al., 1999a; 1999b), it can be seen that the Schmidt method is performed satisfactorily if the first ten terms of infinite series in Eq. (31) are retained. The behavior of the sum of the series keeps steady with the increasing number of terms in (31). The constants of materials-I are assumed to be that (Song and Sih, 2003; Huang and Kuo, 1997; Li, 2000) $c_{44}^{(1)}=44.0$ (GPa), $e_{15}^{(1)}=5.8$ (C/m^2), $\varepsilon_{11}^{(1)}=5.64\times10^{-9}$ (C^2/N m^2), $q_{15}^{(1)}=275.0$ (N/A m), $d_{11}^{(1)}=0.005\times10^{-9}$ (N s/V C), $\mu_{11}^{(1)}=-297.0\times10^{-6}$ (N s^2/C^2), $\rho^{(1)}=1500$ kg/m^3. The constants of materials-II are assumed to be that $c_{44}^{(2)}=54.0$ (GPa), $e_{15}^{(2)}=7.8$ (C/m^2), $\varepsilon_{11}^{(2)}=3.64\times10^{-9}$ (C^2/N m^2), $q_{15}^{(2)}=175.0$ (N/A m), $d_{11}^{(2)}=0.008\times10^{-9}$ (N s/V C), $\mu_{11}^{(2)}=-197.0\times10^{-6}$ (N s^2/C^2), $\rho^{(2)}=2000$ kg/m^3. The constants of materials-III are assumed to be that $c_{44}^{(2)}=34.0$ (GPa), $e_{15}^{(2)}=4.8$ (C/m^2), $\varepsilon_{11}^{(2)}=4.64\times10^{-9}$ (C^2/N m^2) , $q_{15}^{(2)}=195.0$ (N/A m), $d_{11}^{(2)}=0.004\times10^{-9}$ (N s/V C), $\mu_{11}^{(2)}=-201.0\times10^{-6}$ (N s^2/C^2), $\rho^{(2)}=1000$ kg/m^3. At $-l\leqslant x\leqslant l,\ y=0$, it can be obtained that $\tau_{yz}^{(1)}/\tau_0$ is very close to negative unity. Hence, the solution of present paper can also be proved to satisfactory the boundary conditions (1). The numerical results of the present paper are shown in Figs. 2–11.

From the results, the following observations are very significant:

(i) As discussed in the works (Zhou et al., 2004), the stress intensity factor does not depend on the properties of the material for the anti-plane shear static fracture problem in piezoelectric/piezomagnetic materials. However, the dynamic stress, the electric displacement and the magnetic flux intensity factors not only depend on the crack length, the wave velocity,

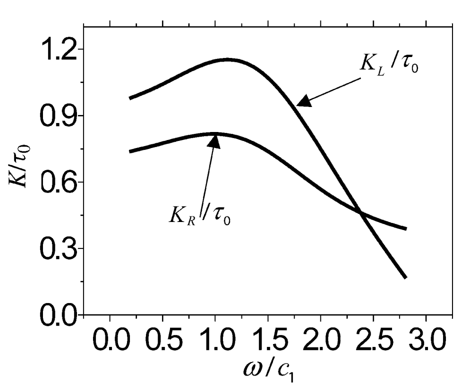

Fig. 2. The stress intensity factor versus ω/c_1 for $b=0.1$ (materials-I/materials-II).

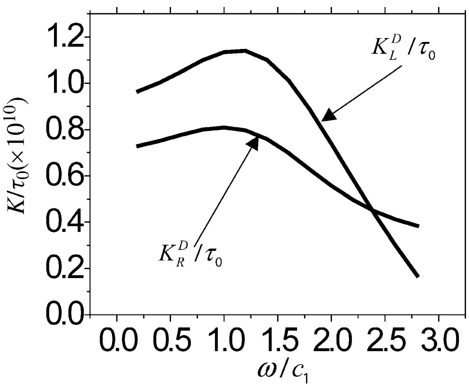

Fig. 3. The electric displacement intensity factor versus ω/c_1 for $b=0.1$ (materials-I/materials-II).

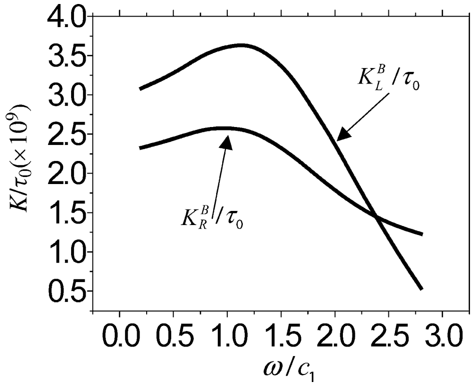

Fig. 4. The magnetic flux intensity factor versus ω/c_1 for $b = 0.1$ (materials-I/materials-II).

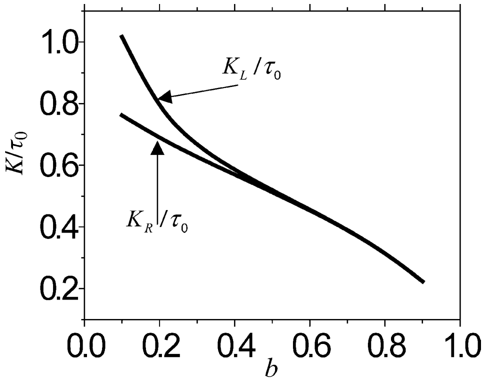

Fig. 5. The stress intensity factor versus b for $\omega/c_1 = 0.4$ (materials-I/materials-II).

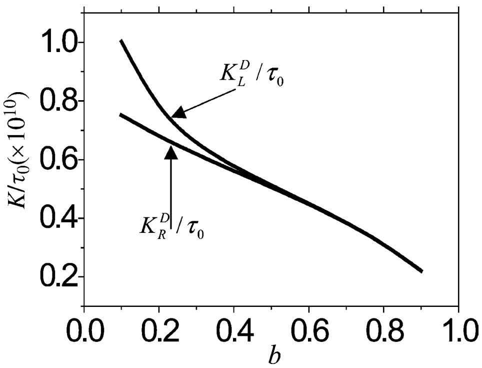

Fig. 6. The electric displacement intensity factor versus b for $\omega/c_1 = 0.4$ (materials-I/materials-II).

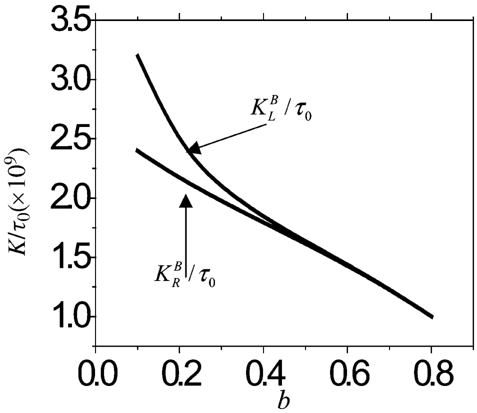

Fig. 7. The magnetic flux intensity factor versus b for $\omega/c_1 = 0.4$ (materials-I/materials-II).

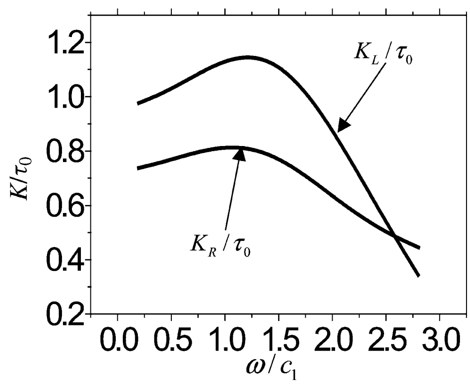

Fig. 8. The stress intensity factor versus ω/c_1 for $b = 0.1$ (materials-I/materials-III).

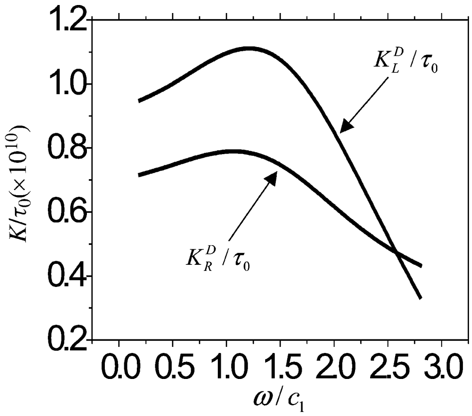

Fig. 9. The electric displacement intensity factor versus ω/c_1 for $b = 0.1$ (materials-I/materials-II).

the circular frequency of the incident waves, but also on the properties of the materials. This is the primary difference between the present paper and the works (Zhou et al., 2004). From the results, it can be shown that the dynamic singular stress in piezoelectric/piezomagnetic materials carries the same forms as those in the general elastic materials. The electro-magneto-elastic coupling effects can be obtained as shown in Eqs. (42)–(47).

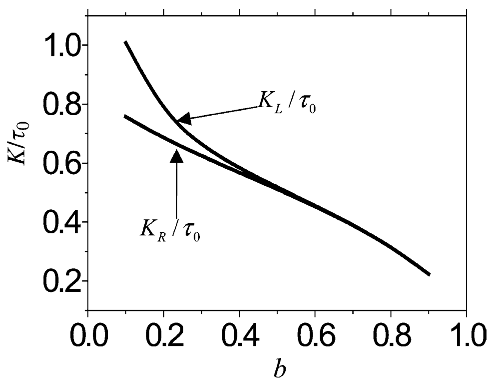

Fig. 10. The stress intensity factor versus b for $\omega/c_1 = 0.4$ (materials-I/materials-III).

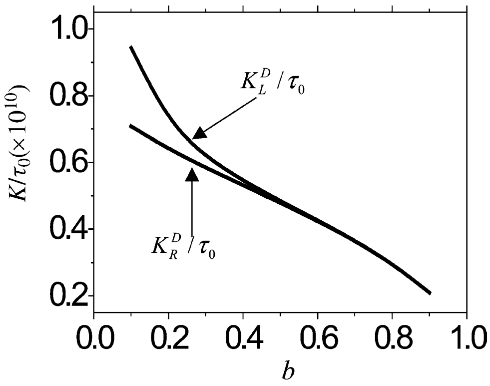

Fig. 11. The electric displacement intensity factor versus b for $\omega/c_1 = 0.4$ (materials-I/materials-III).

(ii) The interaction of the two collinear cracks decrease when the distance between the two collinear cracks increases as shown in Figs. 5–7 and 10, 11. The intensity factors at the inner crack tips are bigger than those at the outer crack tips. However, the intensity factors at the inner and outer crack tips are almost overlapped for $b \geqslant 0.5$ as shown in Figs. 5–7 and 10, 11.

(iii) The dynamic stress intensity factors tend to increase with the frequency reaching a peak and then to decrease in magnitude. In Figs. 2–4 and 8, 9, the intensity factors at the inner crack tips are smaller than those at the outer crack tips for $\omega/c_1 > 2.3$. These phenomena may be caused by the coupling effects among the mechanical, the electric field and the magnetic flux field.

(iv) The variations of K/τ_0, K^D/τ_0 and K^B/τ_0 with ω/c_1 or b have a same tendency as shown in Figs. 2–11. However, the amplitude values of K/τ_0, K^D/τ_0 and K^B/τ_0 are different. The amplitude values of K^D/τ_0 and K^B/τ_0 are very small as shown in Figs. 3, 4, 6, 7, 9 and 11.

Acknowledgements

The authors are grateful for the financial support by the Natural Science Foundation of Hei Long Jiang Province (A0301), the National Natural Science Foundation of China (50232030, 10172030), the National Science Foundation with Excellent Young Investigators (10325208) and the Natural Science Foundation with Excellent Young Investigators of Hei Long Jiang Province.

Appendix

$$[X_1] = \begin{bmatrix} 1 & 0 & 0 \\ \dfrac{a_1}{a_0} & 1 & 0 \\ \dfrac{a_2}{a_0} & 0 & 1 \end{bmatrix}, \quad [X_2] = \begin{bmatrix} -1 & 0 & 0 \\ -\dfrac{a_4}{a_3} & -1 & 0 \\ -\dfrac{a_5}{a_3} & 0 & -1 \end{bmatrix}, \quad [X_3] = \begin{bmatrix} \mu^{(1)}\gamma_1 & se_{15}^{(1)} & sq_{15}^{(1)} \\ 0 & s\varepsilon_{11}^{(1)} & sd_{11}^{(1)} \\ 0 & sd_{11}^{(1)} & s\mu_{11}^{(1)} \end{bmatrix},$$

$$[X_4] = \begin{bmatrix} \mu^{(2)}\gamma_2 & se_{15}^{(2)} & sq_{15}^{(2)} \\ 0 & s\varepsilon_{11}^{(2)} & sd_{11}^{(2)} \\ 0 & sd_{11}^{(2)} & s\mu_{11}^{(2)} \end{bmatrix}, \qquad [X_5] = [X_1] - [X_2][X_4]^{-1}[X_3],$$

$$[X_6] = \begin{bmatrix} -\mu^{(1)}\gamma_1 & -se_{15}^{(1)} & -sq_{15}^{(1)} \\ 0 & s\varepsilon_{11}^{(1)} & sd_{11}^{(1)} \\ 0 & sd_{11}^{(1)} & s\mu_{11}^{(1)} \end{bmatrix},$$

$$[X_7] = \begin{bmatrix} x_{11}(s) & x_{12}(s) & x_{13}(s) \\ x_{21}(s) & x_{22}(s) & x_{23}(s) \\ x_{31}(s) & x_{32}(s) & x_{33}(s) \end{bmatrix} = [X_6][X_5]^{-1}, \qquad g_1(s) = x_{11}(s), \quad g_2(s) = x_{21}(s), \quad g_3(s) = x_{31}(s),$$

$$[Y_3]=\begin{bmatrix}\mu^{(1)} & e_{15}^{(1)} & q_{15}^{(1)}\\ 0 & \varepsilon_{11}^{(1)} & d_{11}^{(1)}\\ 0 & d_{11}^{(1)} & \mu_{11}^{(1)}\end{bmatrix},\qquad [Y_4]=\begin{bmatrix}\mu^{(2)} & e_{15}^{(2)} & q_{15}^{(2)}\\ 0 & \varepsilon_{11}^{(2)} & d_{11}^{(2)}\\ 0 & d_{11}^{(2)} & \mu_{11}^{(2)}\end{bmatrix},$$

$$[Y_5]=[X_1]-[X_2][Y_4]^{-1}[Y_3],\qquad [Y_6]=\begin{bmatrix}-\mu^{(1)} & -e_{15}^{(1)} & -q_{15}^{(1)}\\ 0 & \varepsilon_{11}^{(1)} & d_{11}^{(1)}\\ 0 & d_{11}^{(1)} & \mu_{11}^{(1)}\end{bmatrix},$$

$$[Y_7]=\begin{bmatrix}y_{11} & y_{12} & y_{13}\\ y_{21} & y_{22} & y_{23}\\ y_{31} & y_{32} & y_{33}\end{bmatrix}=[Y_6][Y_5]^{-1},\quad \beta_1=y_{11},\quad \beta_2=y_{21},\quad \beta_3=y_{31}.$$

References

Avellaneda, M., Harshe, G., 1994. Magnetoelectric effect in piezoelectric/magnetostrictive multiplayer (2–2) composites. J. Intelligent Material Systems and Structures 5, 501–513.

Benveniste, Y., 1995. Magnetoelectric effect in fibrous composites with piezoelectric and magnetostrictive phases. Phys. Rev. B 51, 16424–16427.

Erdelyi, A. (Ed.), 1954. Tables of Integral Transforms, vol. 1. McGraw-Hill, New York, pp. 34–89.

Gao, C.F., Kessler, H., Balke, H., 2003a. Fracture analysis of electromagnetic thermoelastic solids. Eur. J. Mech. A Solids 22 (3), 433–442.

Gao, C.F., Kessler, H., Balke, H., 2003b. Crack problems in magnetoelectroelastic solids. Part I: Exact solution of a crack. Int. J. Engrg. Sci. 41 (9), 969–981.

Gao, C.F., Kessler, H., Balke, H., 2003c. Crack problems in magnetoelectroelastic solids. Part II: General solution of collinear cracks. Int. J. Engrg. Sci. 41 (9), 983–994.

Gao, C.F., Tong, P., Zhang, T.Y., 2003d. Interfacial crack problems in magneto-electroelastic solids. Int. J. Engrg. Sci. 41 (18), 2105–2121.

Gradshteyn, I.S., Ryzhik, I.M. (Eds.), 1980. Table of Integrals, Series and Products. Academic Press, New York. pp. 1035–1037.

Harshe, G., Dougherty, J.P., Newnham, R.E., 1993. Theoretical modeling of 3-0/0-3 magnetoelectric composites. Int. J. Appl. Electromagn. Mater. 4, 161–171.

Huang, J.H., Kuo, W.S., 1997. The analysis of piezoelectric/piezomagnetic composite materials containing ellipsoidal inclusions. J. Appl. Phys. 81 (3), 1378–1386.

Li, J.Y., 2000. Magnetoelectroelastic multi-inclusion and inhomogeneity problems and their applications in composite materials. Int. J. Engrg. Sci. 38, 1993–2011.

Liu, J.X., Liu, X.L., Zhao, Y.B., 2001. Green's functions for anisotropic magnetoelectroelastic solids with an elliptical cavity or a crack. Int. J. Engrg. Sci. 39 (12), 1405–1418.

Morse, P.M., Feshbach, H., 1958. Methods of Theoretical Physics, vol. 1. McGraw-Hill, New York. p. 926.

Nan, C.W., 1994. Magnetoelectric effect in composites of piezoelectric and piezomagnetic phases. Phys. Rev. B 50, 6082–6088.

Sih, G.C., Song, Z.F., 2003. Magnetic and electric poling effects associated with crack growth in $BaTiO_3$–$CoFe_2O_4$ composite. Theoret. Appl. Fracture Mech. 39, 209–227.

Soh, A.K., Fang, D.N., Lee, K.L., 2000. Analysis of a bi-piezoelectric ceramic layer with an interfacial crack subjected to anti-plane shear and in-plane electric loading. Eur. J. Mech. A Solids 19, 961–977.

Song, Z.F., Sih, G.C., 2003. Crack initiation behavior in magnetoelectroelastic composite under in-plane deformation. Theoret. Appl. Fracture Mech. 39, 189–207.

Spyropoulos, C.P., Sih, G.C., Song, Z.F., 2003. Magnetoelectroelastic composite with poling parallel to plane of line crack under out-of-plane deformation. Theoret. Appl. Fracture Mech. 39 (3), 281–289.

Van Suchtelen, J., 1972. Product properties: a new application of composite materials. Phillips Res. Rep. 27, 28–37.

Wang, B.L., Mai, Y.W., 2003. Crack tip field in piezoelectric/piezomagnetic media. Eur. J. Mech. A Solids 22 (4), 591–602.

Wang, B.L., Mai, Y.W., 2004. Fracture of piezoelectromagnetic materials. Mech. Res. Commun. 31 (1), 65–73.

Wu, T.L., Huang, J.H., 2000. Closed-form solutions for the magnetoelectric coupling coefficients in fibrous composites with piezoelectric and piezomagnetic phases. Int. J. Solids Structures 37, 2981–3009.

Yan, W.F., 1967. Axisymmetric slipless indentation of an infinite elastic cylinder. SIAM J. Appl. Math. 15 (2), 219–227.

Zhou, Z.G., Han, H.C., Du, S.Y., 1999a. Investigation of a crack subjected to anti-plane shear by using the non-local theory. Int. J. Solids Structures 36, 3891–3901.

Zhou, Z.G., Bai, Y.Y., Zhang, X.W., 1999b. Two collinear Griffith cracks subjected to uniform tension in infinitely strip. Int. J. Solids Structures 36, 5597–5609.

Zhou, Z.G., Wang, B., Sun, Y.G., 2004. Two collinear interface cracks in magneto-electro-elastic composites. Int. J. Engrg. Sci. 42 (11–12), 1155–1167.

Zhou, Z.G., Wang, B., Cao, M.S., 2001. Analysis of two collinear cracks in a piezoelectric layer bonded to dissimilar half spaces subjected to anti-plane shear. Eur. J. Mech. A Solids 20, 213–226.